DocuSign Envelope ID: 38D0E95E-DD99-44C8-8D42-44CE83DC948B

KINETICS OF DARK ADAPTATION IN FORMER PRETERMS

A thesis presented to the graduate faculty of New England College of Optometry in partial fulfillment of the requirements for the degree of Master of Science.

Chung Ki (Kristi) Fung, OD

December – 2021

©Chung Ki (Kristi) Fung

All rights reserved.

The author hereby grants New England College of Optometry permission to reproduce and to distribute publicly paper and electronic copies of the thesis document in whole or in part.

DocuSign Envelope ID: 38D0E95E-DD99-44C8-8D42-44CE83DC948B

KINETICS OF DARK ADAPTATION IN FORMER PRETERMS

Chung Ki (Kristi) Fung, OD

This manuscript has been read and accepted by the Thesis Committee in satisfaction of the thesis requirements for the degree of Master of Science.

2/15/2022

Date

DocuSigned by:
Anne Fulton
BAFAF099E5A94A6...

Anne Fulton, MD

Graduate Faculty Advisor

Boston Children's Hospital, Harvard Medical School

2/15/2022

Date

DocuSigned by:
Ronald Hansen
05729E330E4B43F...

Ronald Hansen, PhD

Graduate Faculty Advisor & External Examiner

Boston Children's Hospital, Harvard Medical School

2/15/2022

Date

DocuSigned by:
78A8AD972399447...

Thanasis Panorgias, MSc, PhD, FAAO

Internal Examiner

New England College of Optometry

2/15/2022

Date

DocuSigned by:
Jane Gwiazda
3012B96081414B5...

Jane Gwiazda, PhD

Direct of Graduate Studies & Internal Examiner

New England College of Optometry

New England College of Optometry

DocuSign Envelope ID: 38D0E95E-DD99-44C8-8D42-44CE83DC948B

Abstract

Kinetics of Dark Adaptation in Former Preterms

Chung Ki (Kristi) Fung, OD

New England College of Optometry, 2021

Purpose: Rod photoreceptors are known to be involved in the retinopathy of prematurity (ROP) disease process. Dark adaptation is dependent upon biochemical processing between the photoreceptors and pigment epithelium. We studied the recovery of retinal sensitivity at two eccentricities, 10° and 30°. Rod mediated dark-adapted thresholds at 10° have been previously shown to be elevated in some children with a history of ROP.

Methods: Dark adaptation was studied at 10° and 30° in 16 former preterms children (ages 12 – 21 years old) and 18 term-born controls (ages 13-25 years old), in two test sessions. Subjects were dark-adapted for thirty minutes, followed by measurement of dark-adapted thresholds in the temporal retina. A five-minute light exposure estimated to bleach 50% of rhodopsin was delivered and the recovery of thresholds was measured for at least thirty-five minutes. The recovery of rod mediated sensitivity was expressed as the slope, S2 [Lamb & Pugh, 2006]. SPSS was used for statistical analysis, $\alpha = 0.05$.

Results: The recovery of rod mediated sensitivity, summarized by the S2 function of Lamb and Pugh, was the same in former preterms compared to term-born controls. There was no difference in recovery of S2 between 10° and 30° in all participants. Prebleach and postbleach rod mediated dark-adapted thresholds were the same between former preterms and term-born controls. There was a significantly lower prebleach and postbleach rod mediated dark-adapted threshold at 30° compared to 10° in all participants.

DocuSign Envelope ID: 38D0E95E-DD99-44C8-8D42-44CE83DC948B

Conclusions: Our results demonstrated the feasibility of investigating the dark adaptation in former preterms. No significant difference was found between former preterms and term-born controls for S2. Studying dark adaptation contributes to the current understanding of how rod photoreceptor functions are affected in ROP. Dark adaptation and recovery of rod mediated sensitivity could be used as a non-invasive test to monitor potential therapeutic interventions.

DocuSign Envelope ID: 38D0E95E-DD99-44C8-8D42-44CE83DC948B

Acknowledgements

I would like to thank my thesis advisors, Dr. Anne Fulton and Dr. Ronald Hansen of Boston Children's Hospital, Harvard Medical School. They always had an open door whenever I had any questions or needed guidance on my project. Thank you for the high level of autonomy I had to formulate my project. I appreciate your guidance to ensure I was on the right track to meet the goals of my project and understanding that I was in a dual degree program.

I would also like to thank members of my thesis committee who were involved in reviewing and validating my project: Dr. Thanasis Panorgias and Dr. Jane Gwiazda at the New England College of Optometry. Without your participation and input, the validation of this project could have not been successfully conducted.

I would also like to thank members of the Infant Vision lab for all your help throughout the process of my project: Dr. James Akula, Dr. Ramamirtham Ramkumar, Hanna De Bruyn, Amber Curran, Bridget Peterson, and fellow co-op students (Aimee Sun, Stephen Chan, Kenny Huang, Victoria Selian, Nebyou Mergia, Megan Rabins, and Annie Lancos). I am grateful for your assistance in recruitment and administrative support.

Finally, I must express my gratitude to my parents, family, fiancé, and friends for providing me with unfailing support and continuous encouragement throughout my years of study, research, and thesis writing. This accomplishment would not be successful without any of them. Thank you.

Chung Ki (Kristi) Fung

DocuSign Envelope ID: 38D0E95E-DD99-44C8-8D42-44CE83DC948B

Table of Contents

List of Figures and Tables 1
General Introduction 1
1.1 Preterms and Retinopathy of Prematurity 1
1.2 Treatment and Complications of ROP 1
1.3 Causes of ROP 1
1.4 Onset of ROP and Rod photoreceptors 2
1.5 Importance of Rods 2
1.6 Psychophysical Experiment of Rod Function in ROP 3
1.7 Selection of 10° and 30° 3
1.8 Dark Adaptation 5
1.9 Experimental Purpose 6
Methods 7
2.1 Participants 7
2.2 ColorDome Apparatus & Stimuli 11
2.3 Dark adaptation protocol 13
2.4 Analysis 15
Results 16
3.1 S2 function 16
3.2 Rod mediated Dark-Adapted Thresholds 19
3.3 Cone Mediated Dark-Adapted Thresholds 23
4. General Discussion and Conclusions 23
4.1 Summary of Key Findings 23
4.2 S2 rod mediated recovery 24
4.3 S2 Rod Mediated Recovery Literature Comparison 25
4.4 Rod Mediated Thresholds Between Preterms and Term-born Controls 28
4.5 Rod Mediated Thresholds Between 10° and 30° 29
4.6 Cone Mediated Thresholds 29
4.7 Limitations of the study 30
4.8 Strengths 30
4.9 General Conclusion 31
5. Bibliography 33

DocuSign Envelope ID: 38D0E95E-DD99-44C8-8D42-44CE83DC948B

List of Figures and Tables

Figure 1: Widefield enhanced depth optical coherence tomography (OCT) of a retina of a healthy participant 3
Figure 2: Classic work by Hecht et al., 1937 on dark adaptation following five levels of bleach. 5
Table 1: Characteristic of former preterms participants. 8
Figure 3: Reference for classification of ROP 8
Table 2: Characteristics of all participants at time of test 9
Figure 4: Experimental apparatus 11
Figure 5: Raw threshold responses of the right eye following 3.17 log cd/m^2 bleach of Subject K.F 11
Figure 6: Timeline of the experimental protocol 13
Figure 7: S2 at 10° and 30°eccentricity in former preterms 17
Figure 8: S2 at 10° and 30°eccentricity in term-born controls 18
Table 3: ANOVA of S2 function 18
Figure 9: Prebleach and postbleach rod mediated dark-adapted thresholds in former preterms at 10° and 30° 20
Figure 10: Prebleach and postbleach rod mediated dark-adapted thresholds in term-born controls at 10° and 30° 21
Figure 11: Prebleach and postbleach rod mediated dark-adapted thresholds in former preterms by ROP severity at 10° and 30° 22
Table 4: ANOVA of prebleach rod mediated dark-adapted thresholds 23
Table 5: ANOVA of postbleach rod mediated dark-adapted thresholds 23
Figure 12: Stimulus Diameter S2 Literature Comparison 26
Figure 13: Retinal Eccentricity S2 Literature Comparison 27

DocuSign Envelope ID: 38D0E95E-DD99-44C8-8D42-44CE83DC948B

General Introduction

1.1 Preterms and Retinopathy of Prematurity

Advances in neonatology has increased survival rates of preterms and cases of ROP (Kong *et al.*, 2012). In the United States, retinopathy of prematurity (ROP) remains one of the leading causes of visual impairment in infants born preterm (<37 weeks) (Glass et al., 2015). Full term is 38-41 weeks gestation (Glass et al., 2015). ROP is a neurovascular disease that is active during infancy, characterized by abnormal retinal vasculature growth (Hansen et al., 2017). Fortunately, not all preterms are diagnosed with ROP. In 90% of those diagnosed, ROP resolves spontaneously without intervention in early post-term weeks (Repka et al., 2000; Enriquez et al., 2020).

1.2 Treatment and Complications of ROP

The remaining 10% of ROP individuals who require intervention are treated with laser photocoagulation of the peripheral avascular retina, or by intravitreal injections of anti-VEGF agents (Hardy et al., 2006; Stahl et al., 2018). Individuals diagnosed with severe ROP may have a spectrum of systemic comorbidities and ocular complications that include cerebral dysfunction, and intellectual disabilities, nystagmus, amblyopia, early childhood high myopia, and retinal detachment (Glass et al., 2015; Jacobson et al., 2020; Siatkowski et al., 2013; Chan-Ling et al., 2018; Darwish et al., 2018; Enriquez et al., 2020).

1.3 Causes of ROP

Infants are recommended to be screened for ROP in the Neonatal Intensive Care Unit (NICU) if birth weight ≤1500g, gestation age ≤30 weeks, or by recommendation of a pediatrician or neonatologist (Fierson et al., 2018). Multiple risk factors and potential causes have been identified including but not limited to: low birth weight, low gestational age at birth, and fluctuations in oxygen levels while the infant was in the NICU (Khosnoud *et al.*, 2019). While

DocuSign Envelope ID: 38D0E95E-DD99-44C8-8D42-44CE83DC948B

oxygen has been identified as a controllable environmental factor, the incident of ROP persists likely due to the survival of preterms (Gantz et al., 2020).

1.4 Onset of ROP and Rod photoreceptors

Rod photoreceptors, with the exception of the foveal cones, are the last retinal cells to reach maturity (Hendrickson and Drucker, 1992). ROP onset at preterm ages is coincident with rapid developmental elongation of the rhodopsin bearing rod outer segment and the rapid increase of rhodopsin content of the retina (Fulton *et al.,* 1999; Hendrickson and Drucker, 1992; Fulton *et al.*, 2009 a; Hansen *et al.,* 2017). The coincidence of ROP onset and rod development is associated with demonstrable involvement of the rods in the ROP disease process (Fulton *et al.,* 1999; Hansen *et al.,* 2017).

1.5 Importance of Rods

The retina has two classes of photoreceptors, rods and cones. Rod photoreceptors are far more numerous than cones and are distributed throughout the retina except at the very center, the fovea (Provis and Hendrickson, 2008). Rods are ideal for detecting photons, even single photons, in the dark and in dimly lit environments (Kawamura and Tachibanaki, 2008). The cones are also distributed throughout the retina, catch photons in well-lit environments and mediate color vision (Kawamura and Tachibanaki, 2008). At the fovea there are many cones per unit area, ideal for mediating fine visual acuity; the normal foveal center contains no rods (Provis and Hendrickson, 2008). With exception of the foveal cones, maturation of cones antedates that of the rods (Provis and Hendrickson, 2008). The later maturing rods appear to participate in the ROP disease process and to be particularly vulnerable to ROP related injury (Fulton *et al.,* 1999; Hansen *et al.,* 2017). In the context of the present project, the development of the near central rods at 10° is even more delayed than that of more peripheral rods at 30° (Hendrickson and Drucker, 1992). The course of foveal cone development continues for several years after term (Lee *et al.,* 2015)

DocuSign Envelope ID: 38D0E95E-DD99-44C8-8D42-44CE83DC948B

1.6 Psychophysical Experiment of Rod Function in ROP

Results of full field electroretinographic (ERG) studies of dark-adapted eyes have shown low rod sensitivity in individuals with ROP even if ROP regressed spontaneously, that is, without treatment (Fulton et al., 2009 a). Dark-adapted visual thresholds measured using psychophysical procedures allows testing of tiny retinal regions compared to full field ERG that tests the whole retina (Fulton et al., 1996 b). The course of development of the photoreceptors is not uniform across the retina.

1.7 Selection of 10° and 30°

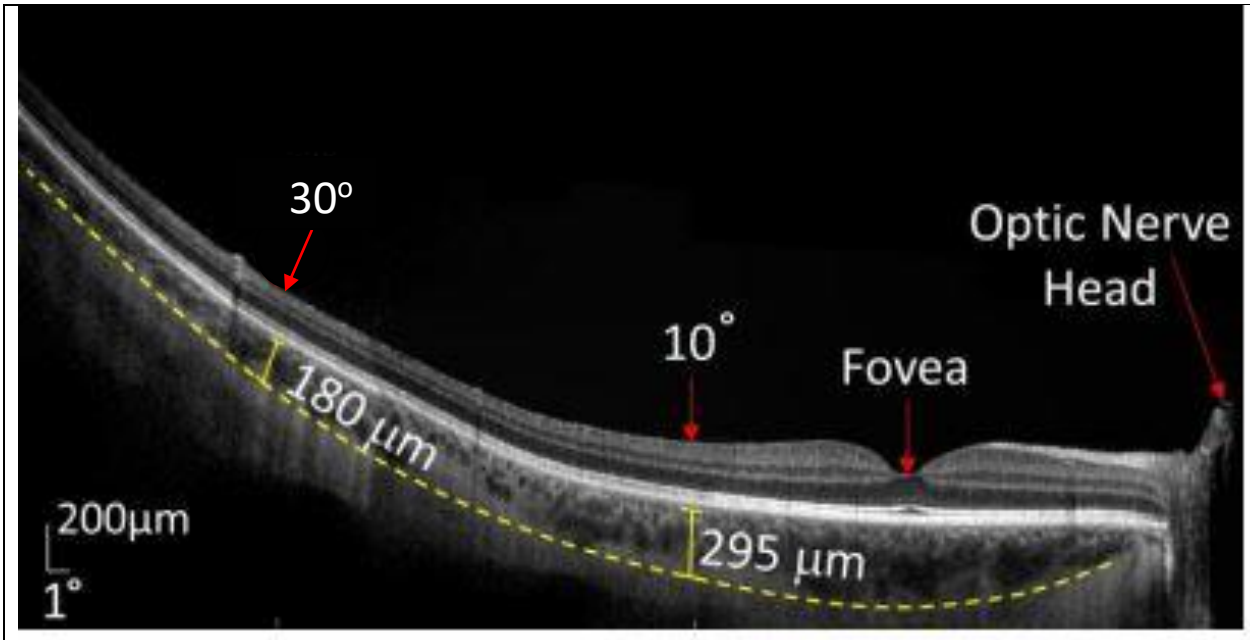

Figure 1: Widefield enhanced depth optical coherence tomography (OCT) of a retina of a healthy participant

OCT using SD-OCT (Spectralis) in a healthy emmetropic individual. The image captures the optic nerve head to ≥35° temporal retina. The optic nerve head, fovea, 10°, and 30° retinal locations are specified with respective red arrows. Choroidal limits are represented by the yellow dashed lines with the respective estimated choroidal thickness reported at 10° and 30°.

We selected 10° and 30° retinal eccentricity for this study based on knowledge of normal retinal development, and the previously demonstrated differential effect of ROP on the dark-adapted visual thresholds mediated by the rods at the two eccentricities. A wide-field enhanced depth retinal OCT of a healthy eye shown in Figure 1 demonstrates 10° and 30° retinal

DocuSign Envelope ID: 38D0E95E-DD99-44C8-8D42-44CE83DC948B

eccentricity. Anatomic studies document delayed developmental elongation of the rod outer segments in the central retina, that includes 10° retinal eccentricity, compared to more peripheral retina, that includes 30° retinal eccentricity (Hendrickson and Drucker, 1992). Parallel with the anatomic development, the normal development of rod mediated thresholds at 10° is delayed compared that of thresholds at 30° (Fulton *et al.*, 1996 a; Hansen *et al.*, 2017).

In infants with a history of ROP compared to healthy term-born infants, there is an even more prolonged course of threshold development at 10°, but not 30° (Barnaby *et al.*, 2007). Interestingly, among children with a history of ROP and early high myopia, elevated threshold at 10° persisted thorough childhood and adolescence (Reisner *et al.*, 1997; Hansen *et al.*, 2017). Individuals with a history of ROP but no early high myopia do not have elevated thresholds at 10°; healthy term-born individuals with high myopia do not have elevated thresholds at 10°. In healthy subjects, the difference in threshold between 10° and 30° was zero (Massof *et al.*, 1981; Hansen and Fulton, 1999; Fulton *et al.*, 2009 b). Bowl et al., (2019) studied dark adaptation in former preterms at 12° retinal eccentricity and found impaired dark adaptation as associated with “arrested foveal development”.

In view of the evidence of ROP involving the rods, we acknowledge the adjacent choroid, the supplier of oxygen to the photoreceptors (Hansen and Fulton, 1995). In preterms, the choroid may be too thin to support rod photoreceptor development (Anderson *et al.*, 2014). Lack of choroidal oxygen delivery along with oxygen fluctuations in the NICU could influence photoreceptor development, in addition to the widely reported altered expression of retinal growth factors, leading to abnormal retinal vasculature growth, the clinical hallmarks of ROP (Sayman *et al.*, 2016; Jang and Kim, 2020).

DocuSign Envelope ID: 38D0E95E-DD99-44C8-8D42-44CE83DC948B

1.8 Dark Adaptation

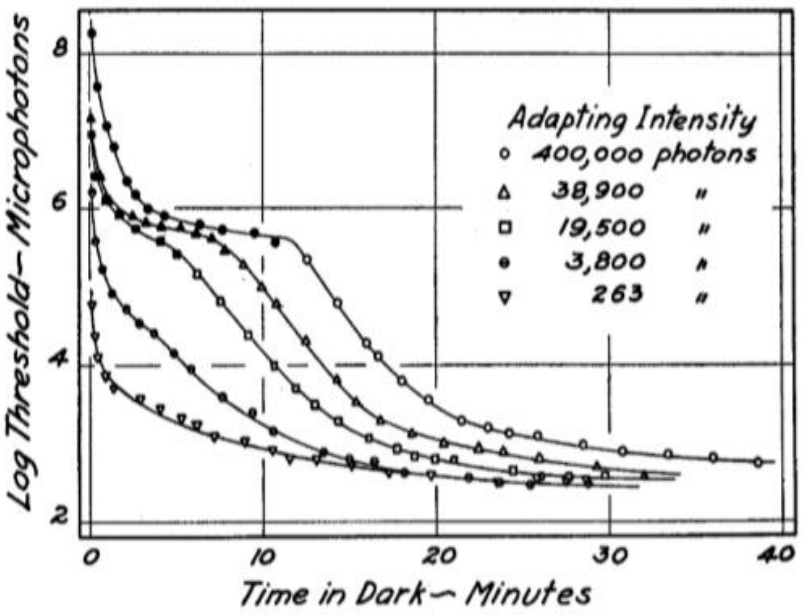

Figure 2: Classic work by Hecht et al., 1937 on dark adaptation following five levels of bleach.

Classic work by Hecht et al., measurement of dark-adapted thresholds (microphotons) as a function of time following five levels of bleach. After a ten-to-fifteen-minute dark adaptation and two-minute light adaptation, a 0.2 second stimulus was presented at 30° on the nasal retina.

The processes by which visual threshold returns to baseline is termed “dark adaptation”. A classic dark-adaptation experiment (Figure 2) showed the effect of five levels of bleach on rod mediated thresholds at 30° nasal retina (Hecht *et al.*, 1937). Bleaching is accomplished by exposing the retina to bright light; photons are absorbed by visual pigments, such as rhodopsin (Lamb, 1981). Visual thresholds become elevated following a bleach (Hecht *et al.*, 1937; Mahroo and Lamb, 2004). The process of converting the light detection to neural processing begins in the outer segments of the photoreceptors. This process is limited by the rate of 11- cis retinal (chromophore) in the retinal pigment epithelium delivered to rhodopsin (opsin) in rod photoreceptors (Lamb and Pugh, 2004; Palczewski, 2006). Following fairly large bleaches, there are two distinct regions of the biphasic dark adaptation curve: a cone mediated phase and a rod mediated phase.

DocuSign Envelope ID: 38D0E95E-DD99-44C8-8D42-44CE83DC948B

The cone mediated phase begins immediately after a bleach. In the "400,000 photon" example shown in Figure 2, cone mediated dark-adapted thresholds decreased approximately 2 log units over the next 10 minutes (Hecht et al., 1937). After the cone mediated phase, the rod mediated phase is seen as the retina becomes capable of detecting dimmer and dimmer light (Hecht et al., 1937). Depending on specific experimental conditions, the rod mediated phase may take approximately 50 to 60 minutes to recover to pre-bleach threshold levels (Leibrock *et al.*, 1998). Lamb (1981) was the first to note that the recovery of rod mediated sensitivity could be summarized by a line fitted to log thresholds as a function of linear time. He termed this "S2".

Lamb reported an S2 of -0.24 log unit/min for a wide range of bleach strengths (0.5% to 98%) (1981; Ruseckaite *et al.*, 2011). This slope, S2, depends on regeneration of rhodopsin after a bleach (Lamb, 1981). Previous literature reported slower S2 function and higher visual threshold in various retinal conditions such as Stargardt's, age-related macular degeneration, vitamin A deficiency, and Fundus Albipunctatus, aging (Blakemore and Rushton, 1965; Glenn et al., 1994, Cideciyan *et al.*, 2004; Jackson et al., 1999).

1.9 Experimental Purpose

Previous psychophysical experiments have demonstrated higher dark-adapted thresholds at 10° compared to 30°, in children with a history of ROP and early high myopia (Reisner *et al.*, 1997; Hansen *et al.*, 2017). As mentioned above, S2 at 12° eccentric appears slower than normal in former preterms who also have "arrested foveal development" (Bowl *et al*., 2019). To our knowledge, S2 has not been previously measured in former preterms in greater eccentricities. In this experiment, we aim to study rod mediated dark adaptation, delineating S2 at 10° and 30° in former preterms with and without a history of ROP.

DocuSign Envelope ID: 38D0E95E-DD99-44C8-8D42-44CE83DC948B

We hypothesized that the recovery of S2 would be slower in preterms with a history of ROP if they also had high myopia in early childhood. We expected S2 values of other former preterms would be like those in term-born controls. The slower recovery, lower S2, has been found in other retinal diseases that affect the rods.

Methods

2.1 Participants

Former preterms (*n=16*) aged 11 to 20 years old were recruited (Table 1). They were medically stable (not actively being treated for a chronic or acute illness beyond routine care) at the time of visit, born at or before 32 weeks gestation, had appropriate birth weight for gestation age, and had eye exams by a Boston Children's Hospital ophthalmologist. Subjects were excluded if they had history of structural anomalies of the anterior or posterior segment, anomalies of the brain, retinal surgery not related to ROP, retinal degenerations, and or family history of any heritable retinal disease. In this study, we categorized ROP into 3 different groups: *no ROP* (NROP) former preterms screened but never had ROP, *mild/untreated ROP* (UROP) former preterms diagnosed with ROP that spontaneously regressed without treatment by term, and *severe/treated ROP* (TROP) former preterms diagnosed with ROP and required intervention.

The median gestational age for all former preterm's was 27.5 (25 to 32) weeks with medians shown in Table 1. Median birth weight of all former preterm was 966 (490 – 2015) grams. All former preterms were born between 1999 to 2010. All UROP and TROP participants had bilateral ROP, but only the eye with better visual acuity was tested. There was little difference between the severity of ROP history between eyes. All ROP histories are reported according to the International Classification of ROP; 3rd edition.

DocuSign Envelope ID: 38D0E95E-DD99-44C8-8D42-44CE83DC948B

Table 1: Characteristic of former preterms participants.

		NROP	UROP	TROP
Patients, *n*	**n**	8	7	1
Age, years	**Median**	15	18	12
	Range	11 -21	13 -21	NA
Gestational age, weeks	**Median**	31	26	25
	Range	27 - 32	23 - 28	NA
Birth weight, grams	**Median**	1385	705	490
	Range	1000 - 2015	570 - 931	NA
BCVA, logMAR	**Median**	0.01	0.10	0.00
	Range	-0.06 - +0.10	-0.12 - +0.34	NA
Spherical equivalent, diopters	**Median**	0.00	-0.25	+1.00
	Range	-4.25 - +2.00	-1.50 -+0.75	NA

There was no range for TROP as there was only one TROP included in the study. Spherical equivalent was rounded to the closest 0.25 diopter step.

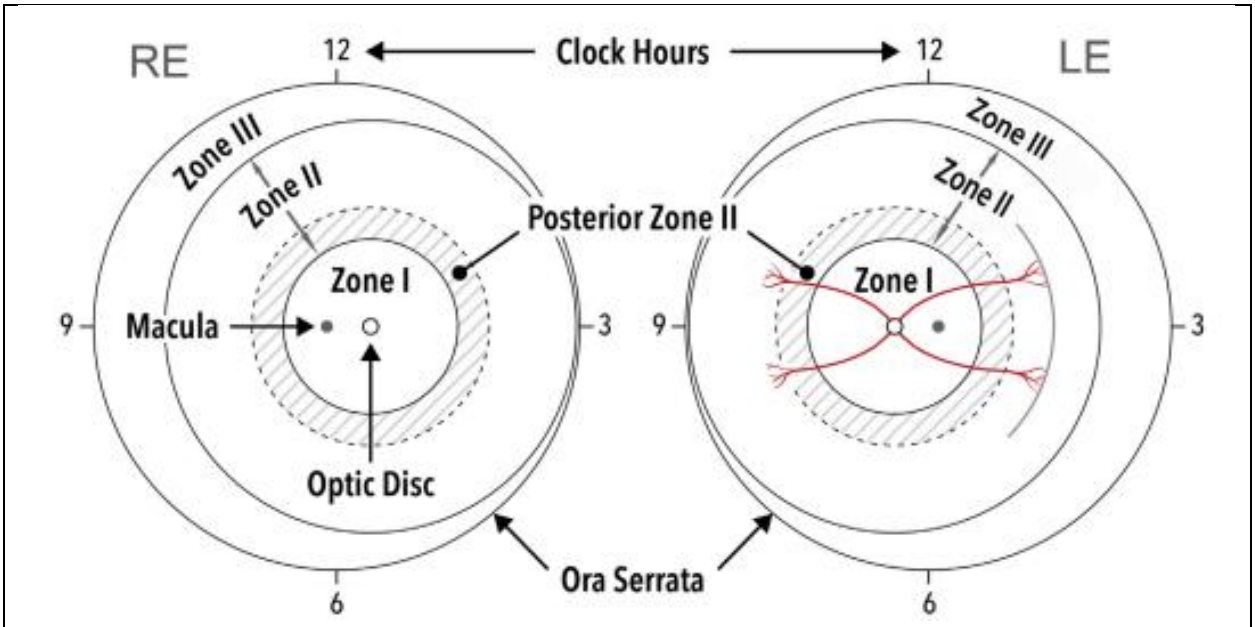

Figure 3: Reference for classification of ROP

Reference guide for the 2021 International Classification of ROP in the right and left eye. Image is from the International Classification of ROP, 3rd edition. Schematic details the zones, clock hours, and other clinical landmarks such as the macula and optic disc. Boundaries of zones are represented by solid lines and posterior pole by dashed lines.

The international classification of ROP classified ROP primarily on three components: zones (location), stages (severity), and clock hour (extent) shown in Figure 3 (Chiang *et al*.,

DocuSign Envelope ID: 38D0E95E-DD99-44C8-8D42-44CE83DC948B

2021). Zones referred to three concentric retinal rings. Zone I was the most posterior region defined by a ring twice the radius from the optic disc center to the foveal center. Zone II was the area from Zone I extending to the ora serrata nasally, temporally, superiorly, and inferiorly. Zone III was the remaining peripheral retina beyond the ora serrata (Chiang *et al*., 2021). Stages referred to vascular hallmarks at the vascular and avascular retina junction. Stage 1's feature was a demarcation line, stage 2 was a ridge, stage 3 was extraretinal neovascular proliferation, stage 4 was partial retinal detachment, and stage 5 was total retinal detachment (Chiang *et al*., 2021). Lastly, clock hours localized the disease to a specific 30° window outlined in Figure 3 (Chiang *et al*., 2021). Additional terms have been included as the classification of ROP has been revised. Terms like plus and preplus disease described the appearance of blood vessels. Plus disease meant dilated and tortuous vessels, and preplus disease meant abnormal vasculature but not to the extent of plus disease (Chiang et al., 2021).

Table 2: Characteristics of all participants at time of test

		Former Preterms	**Term-born controls**	**Significance**
Patients	n	16	18	NA
Age, years	Median	16	22	0.003*
	Range	11 - 21	12 - 25	
BCVA, logMAR	Median	0.01	-0.02	0.425
	Range	-0.12 - +0.34	-0.14 - +0.36	
Spherical Equivalent, diopters	Median	-0.00	-0.75	0.117
	Range	-4.25 - +2.00	-6.00 - +3.00	

Statistical significant is denoted by * ($\alpha = 0.05$). Statistical significance was calculated by T-test. NA means not applicable. Term-born control participants were significantly older than our former preterms. Of the sixteen former preterms, only nine completed both test sessions, and fifteen of our eighteen term-born controls completed both test sessions. Spherical equivalent was rounded to the closest 0.25 diopter step.

All UROPs had a history of ROP in either zone 2 or 3, stage 1 or 2, and one clock hour around the clock (1-12 o clock), no plus disease. The TROP participant had zone 2, stage 3, clock hour 2, preplus disease. Former preterms had a median spherical equivalent of -0.06 (-4.25 to +2.00) diopters, a median visual acuity of 0.01 (-0.12 to 0.34) logMAR (Table 2).

DocuSign Envelope ID: 38D0E95E-DD99-44C8-8D42-44CE83DC948B

Term-born controls (*n=18*) ages 13 – 25 years old were recruited (Table 2). Term-born controls did not have any systemic or ocular disorder and birth was at/or after 37 weeks of gestation. Exclusion criteria were the same as former preterms. Term-born controls had a median spherical equivalent of -0.75 (-6.00 to +3.00) diopters. Term-born controls had a median visual acuity of -0.02 (-0.14 to 0.36) logMAR (Table 2).

Visual acuities and refractive error were measured prior to measurement of dark-adapted thresholds (DAT). Visual acuities were measured with the Early Treatment Diabetic Retinopathy Study (ETDRS) visual acuity chart. Participants stood 10 feet away from the ETDRS chart and were provided with an occluder. Monocular acuities were first taken before binocular acuities. A new ETDRS chart was presented for each eye. Refractive error was measured by WR-5100K autorefractor by Grand Seiko (Hiroshima, Japan). Participants were asked to remove any corrective lenses or contacts and were seated in front of the autorefractor. Participants were asked to keep both eyes open and look at a distant target through the clear window of the autorefractor. Refractive error was taken for each eye as the participant viewed a distant target down a hallway.

DocuSign Envelope ID: 38D0E95E-DD99-44C8-8D42-44CE83DC948B

2.2 ColorDome Apparatus & Stimuli

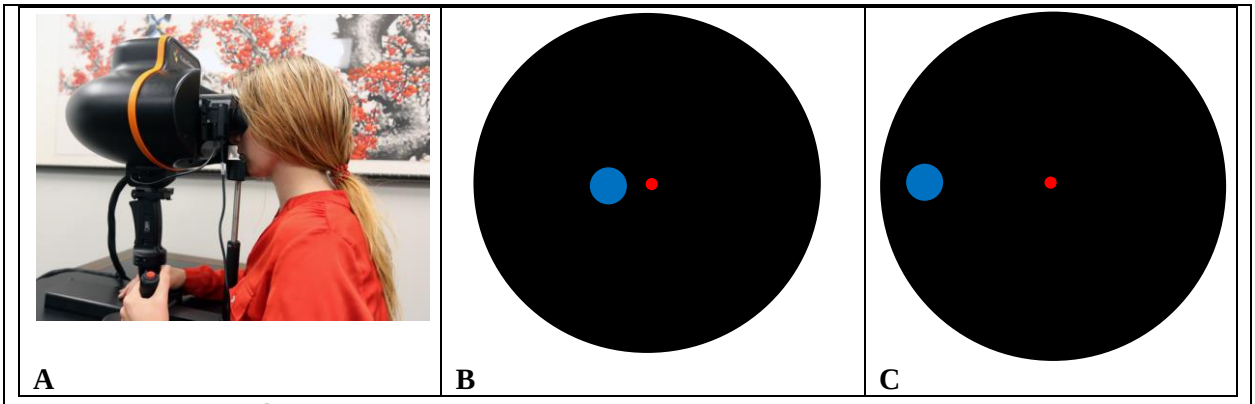

Figure 4: Experimental apparatus

(A) A participant looking into the ColorDome. The image was from the Diagnosys instructions manual. (**B)** Schematic of the subject's right eye view tested at 10°. The small red dot represents the fixation stimulus, and the larger blue dot represents the rod favored testing stimulus. Image was not drawn to scale. **(C)** Schematic of subject's right eye view tested at 30°.

An FDA approved ColorDome by Diagnosys (Espion e^2; Diagnosys; Lowell, USA) (Figure 4A) was used to measure dark-adapted thresholds and rod mediated recovery of sensitivity. A customized iMask was used to control testing diameter, eccentricity, and fixation intensity. The iMask contained one pinhole aperture (~0.25º) to view the fixation stimulus and one 2° diameter aperture at either 10° or 30° to view the test stimulus (Figure 4 B & C). Only the temporal retinal was tested. The expected pattern of a post-bleached threshold response (Figure 5) was composed of a cone mediated response (red circles), rod mediated response (blue triangles), rod absolute threshold plateau, and S2 function (green line). Although the ColorDome was programmed to record rod mediated and cone mediated thresholds, we will primarily be focusing on rod mediated findings.

Test stimulus was a 2º blue ($\lambda = 445 \pm 20$ nm) or red light ($\lambda = 650 \pm 20$ nm) presented at either 10° or 30° for 50 msec in 2 second intervals (Figure 4 B & C). Each test session lasted about two hours, so only one eccentricity was tested per session. Order of eccentricity was randomized for all participants. Blue light favored rod function and red light favored cone function. A customized fixation intensity controller was installed in each iMask. During our pilot studies,

DocuSign Envelope ID: 38D0E95E-DD99-44C8-8D42-44CE83DC948B

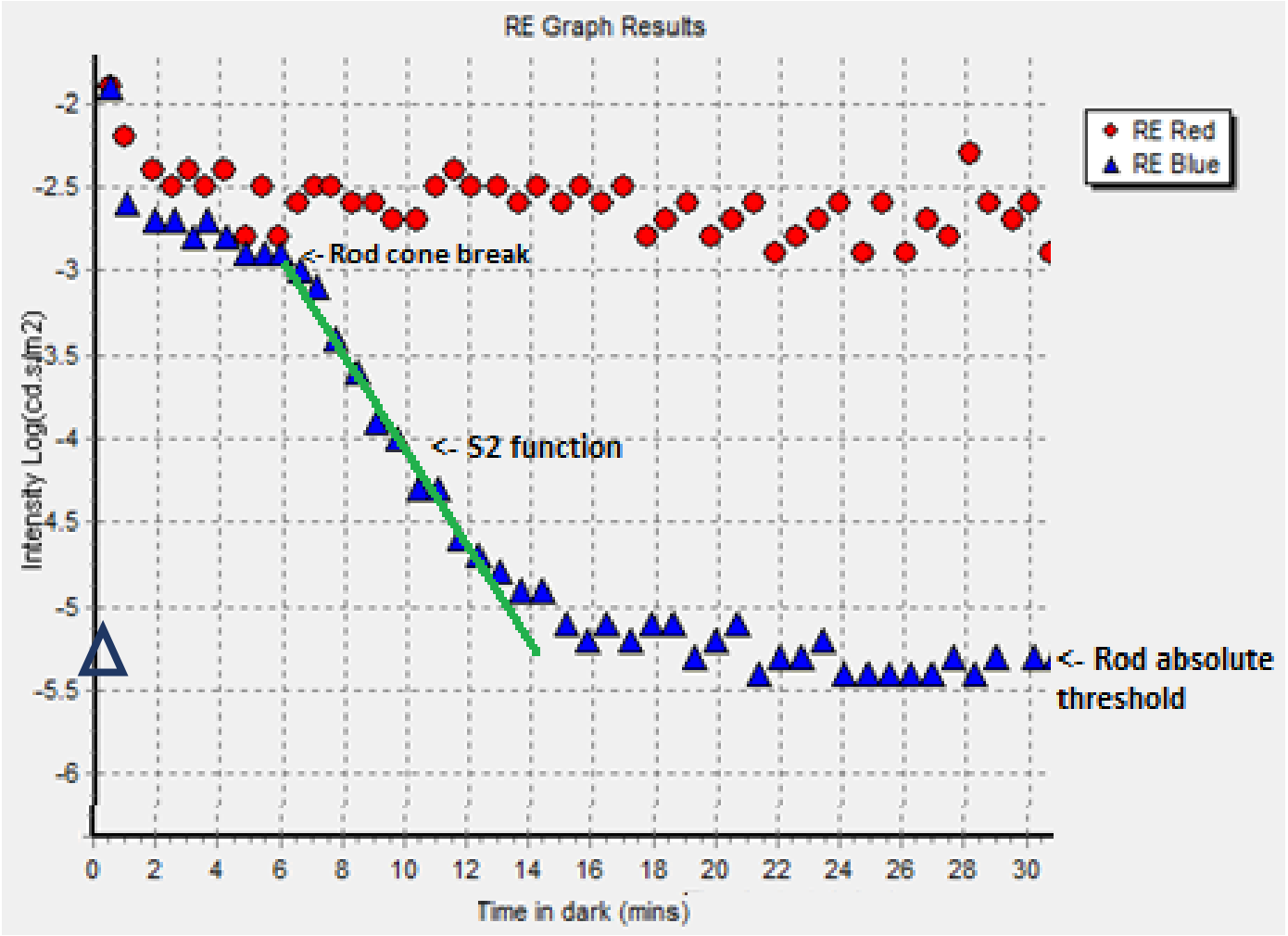

Figure 5: Raw threshold responses of the right eye following 3.17 log cd/m^2 bleach of Subject K.F

Raw dark-adapted thresholds (log (cd.s/m^2) as a function of time. Subject K.F first dark-adapted for thirty minutes then recorded ten minutes of prebleach dark-adapted rod mediated threshold as marked by the open triangle. A five-minute 3.17 log cd/m^2 was delivered, dark-adapted thresholds were measured for at least thirty minutes. Rod mediated thresholds are represented by red circles and cone mediated thresholds by blue triangles. S2 was represented by the

DocuSign Envelope ID: 38D0E95E-DD99-44C8-8D42-44CE83DC948B

participants expressed confusion with fixation and test stimulus during the 10° test session. Participants reported a brighter fixation stimulus masking the test stimulus as thresholds approached baseline. The controller help adjust the intensity of fixation light to avoid bleaching and confusion effects as participants approached baseline visual thresholds.

The fixation stimulus was viewed through a 0.9 neutral density filter to see a pinhole sized red light (λ = 650 nm). Bleaching stimulus was a five-minute full field broad band white light (6500K) of 3.17 log.cd/m^2. A fifteen second "ramp" time was incorporated into the bleach for subject comfort. During the "ramp" time, the bleach started dim and rapidly increased to full bleach intensity.

2.3 Dark adaptation protocol

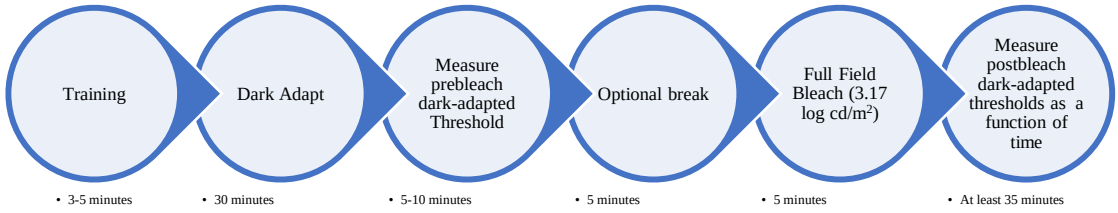

Figure 6*: Timeline of the experimental protocol*

Experimental protocol for subject's DAT.

A timeline of the experimental protocol is outlined in Figure 6. Participants were first trained on the ColorDome DAT procedure for three to five minutes in room light. A response clicker was given to participants to record their responses. A participant's right eye view during 10° and 30° testing is demonstrated in Figures 4B & C respectively. Rod favored stimuli, cone favored stimuli, and fixation stimuli were shown. Participants were asked to always view the fixation stimulus. A rod favored test stimulus was first presented, if the light was seen, participants were asked to press a button on the response clicker. The seen rod mediated

DocuSign Envelope ID: 38D0E95E-DD99-44C8-8D42-44CE83DC948B

threshold would be recorded in the Espion PC. A cone favored test stimulus would then be presented, if the light was seen, participants were asked to press the button again. The cone mediated threshold would be recorded in the Espion PC. The ColorDome would alternate between rod and cone favored stimulus presentations, decreasing in intensity by a "step size" until participants could no longer see the light, a reversal. The next stimulus would be more intense. If the participant saw that light, the following light would decrease in intensity until a reversal. The threshold algorithm used was adaptive binary chop.

In an adaptive binary chop algorithm, an initial stimulus, usually 0 log (cd.s/m^2) would be presented. If the stimulus was seen, the algorithm would decrease the light intensity by "step size" (1.0 log unit) until a reversal. At a reversal, the light would increase in intensity by half of the previous "step size", in this case, it would be 0.50 log units, until participants saw the light. The process of increased and decreased light intensity would continue for the test duration of one minute. The last seen threshold at the end of the test time was recorded as the threshold. After the initial baseline thresholds have been recorded, the next trial would use the previously recorded threshold as the new starting point to bracket.

After the demonstration, the fixation stimulus was set to the lowest possible setting to avoid bleaching effects and confusion. Participants then dark-adapted for thirty minutes outside the ColorDome. Prebleach rod mediated, and cone mediated dark-adapted thresholds were then measured with the ColorDome at either 10° or 30° for five to ten minutes depending on the consistency of the subject's response. Participants with inconsistent threshold responses were tested for the full ten minutes. Consistent threshold response was considered at least three consecutive thresholds within 0.10 log units of each other.

DocuSign Envelope ID: 38D0E95E-DD99-44C8-8D42-44CE83DC948B

Participants were given a five-minute break in room light. The iMask was removed to deliver a full field bright white light (3.17 log cd/m^2) for five minutes. This light was estimated to bleach 30 – 50% of the rhodopsin in a normal healthy eye (Mahroo and Lamb, 2004; Ruseckaite et al., 2011). After the bleach, the iMask was immediately placed back on the ColorDome. The postbleach rod mediated and cone mediated thresholds were measured for at least thirty-five minutes.

2.4 Analysis

S2 was described as a line fitted to log thresholds as a function of linear time in the rod mediated phase of the dark adaptation process (Lamb, 1981). S2 has been demonstrated to last 10 to 18 minutes for bleaches over 22% (Lamb and Pugh, 2004; Reuter, 2011). Individual S2 was determined by repeated linear regression of a moving set of ten consecutive raw data points in the recovery of sensitivity response in excel. Ten points were approximately ten minutes of testing. The set of ten consecutive points that gave the highest goodness of fit (R^2) value was determined to be the individual's S2 function. All participants' S2 started within five minutes of the recovery of sensitivity response. Individual prebleach dark-adapted thresholds were reported as the median of five to ten points in the prebleach response and median of the final ten points in the post recovery response. Each point equals one minute of test time.

SPSS statistical software was used for all analyses. Only the data of participants that completed testing at 10° and 30° were included in our analysis. Of the sixteen former preterms, only nine completed both test sessions, and fifteen of our eighteen term-born controls completed both test sessions. A 2-factor repeated-measures ANOVA was used to analyze S2, rod mediated prebleach thresholds, rod mediated postbleach thresholds, cone mediated prebleach thresholds, and cone mediated postbleach thresholds. The within-subject factor was retinal eccentricity (10°

DocuSign Envelope ID: 38D0E95E-DD99-44C8-8D42-44CE83DC948B

vs 30°). The between-subject factor was group (term-born control vs former preterm). $\alpha = 0.05$ for all ANOVA analyses.

Results

3.1 S2 function

The rate of rod mediated recovery, estimated by S2, did not differ between former preterms (Fig 7A) and term-born controls (Fig 8). Severity of ROP had little impact on S2 (Fig 7B). Furthermore, there was no significant difference between 10° and 30° in all participants. There was also no significant interaction between group and eccentricity. The results of a 2-factor ANOVA for S2 are below (Table 3).

DocuSign Envelope ID: 38D0E95E-DD99-44C8-8D42-44CE83DC948B

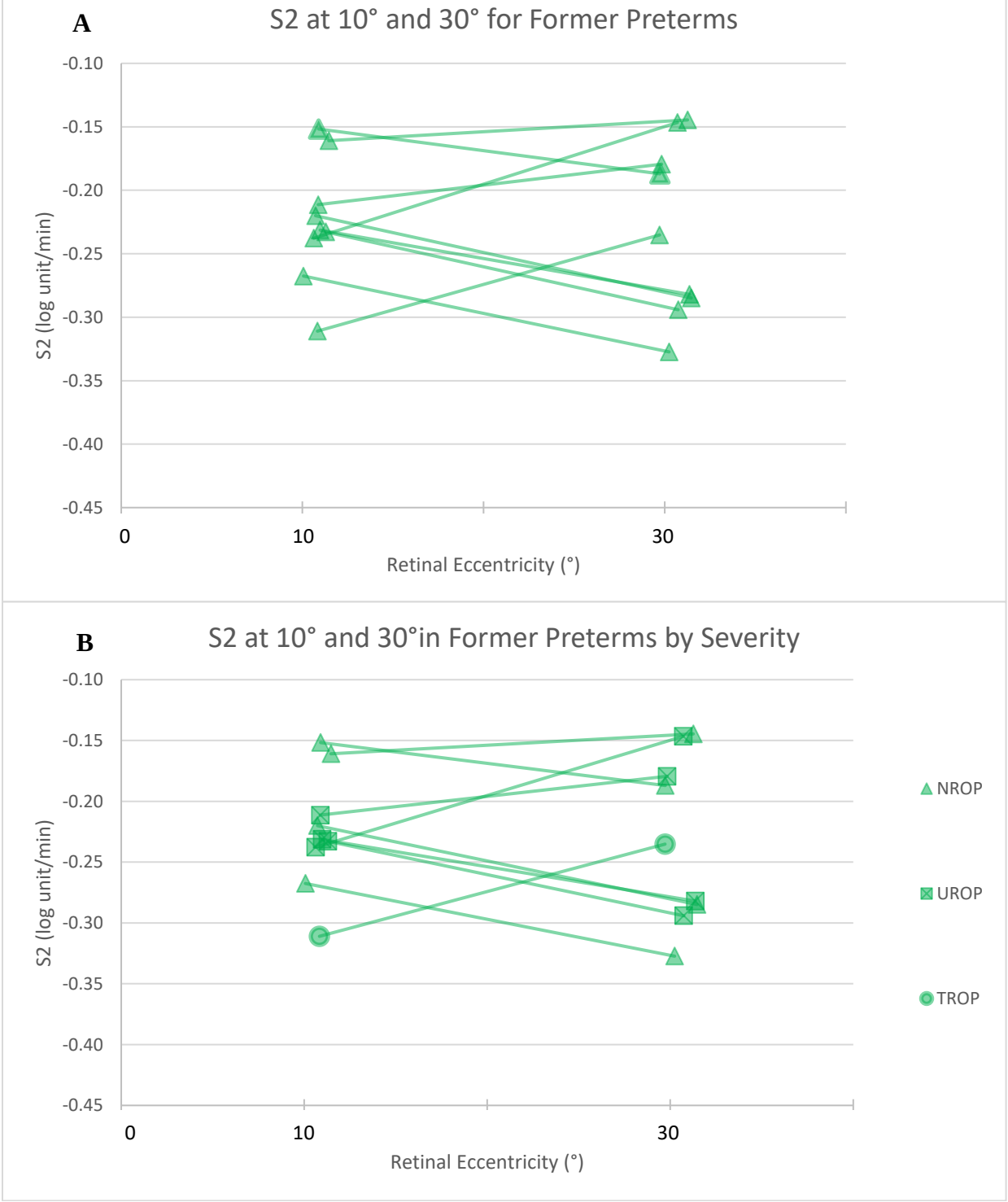

Figure 7: S2 at 10° and 30°eccentricity in former preterms

S2 at 10° and 30° retinal eccentricities in **(A)** former preterms, **(B)** former preterms by ROP severity. Participants who completed both test eccentricities are represented by filled symbols connected by a line. Different symbols indicate the severity of ROP in the former preterms.

DocuSign Envelope ID: 38D0E95E-DD99-44C8-8D42-44CE83DC948B

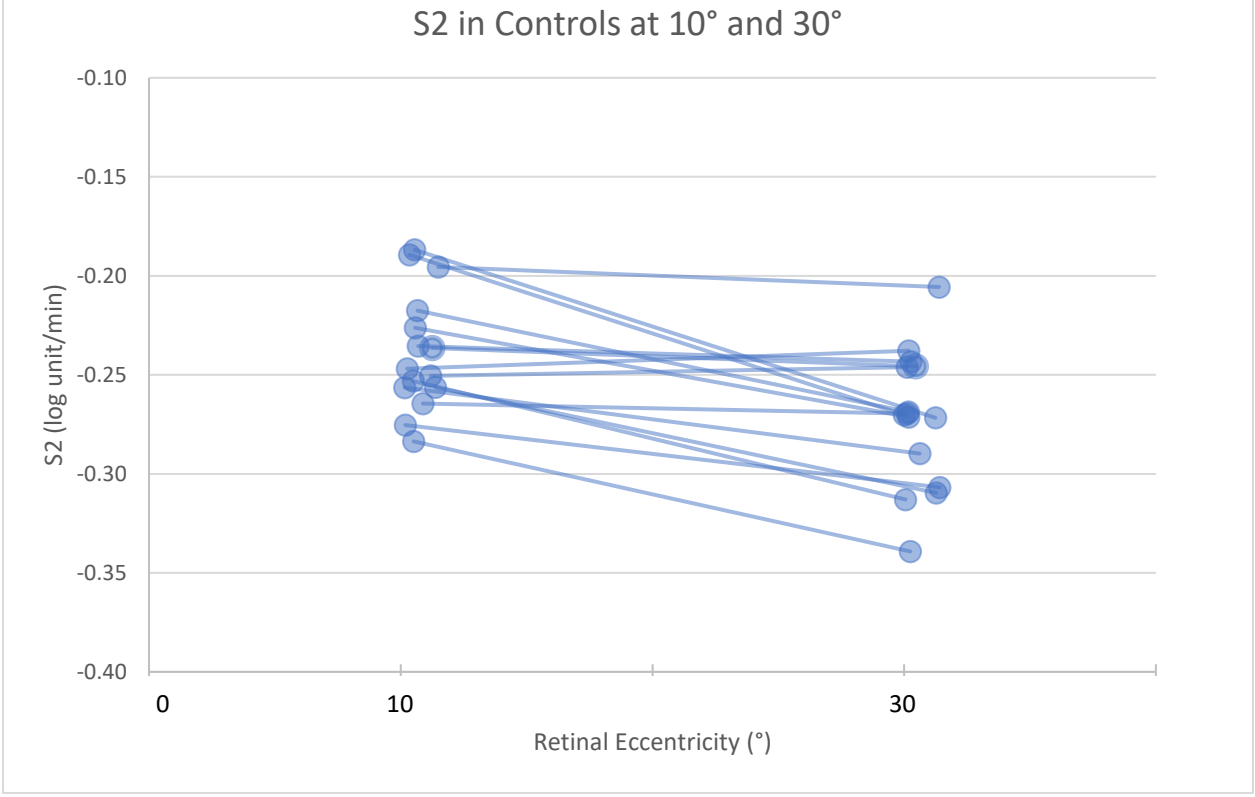

Figure 8: S2 at 10° and 30°eccentricity in term-born controls

S2 at 10° and 30° retinal eccentricity in term-born controls. Participants who completed both test eccentricities are represented by filled symbols connected by a line.

369

Table 3: ANOVA of S2 function

Source	Sum of Squares	df	Mean Square	F	Sig.
Group (Former preterms, Term-born controls)	0.009	1	0.009	3.078	0.094
Eccentricity (10°, 30°)	0.004	1	0.004	3.898	0.062
Group x **Eccentricity**	0.002	1	0.002	1.694	0.207

Statistical significance was denoted by * ($\alpha = 0.05$).

DocuSign Envelope ID: 38D0E95E-DD99-44C8-8D42-44CE83DC948B

3.2 Rod mediated Dark-Adapted Thresholds

Rod mediated dark-adapted thresholds were separated into prebleach and postbleach. There was no significant difference between former preterms (Fig 9A & B) and term born controls (Fig 10A & B) in prebleach and postbleach rod mediated dark-adapted thresholds. Similar to S2 findings, the severity of ROP had little impact on prebleach and postbleach rod mediated dark-adapted thresholds (Fig 11A & B). There was a significant difference of lower threshold responses at 30°, in both prebleach (p=0.000025) and postbleach (p=0.00011) rod mediated dark-adapted thresholds in all participants as demonstrated by the connected lines (Figure 9 and 10). 2-factor ANOVA for prebleach and postbleach rod mediated dark-adapted thresholds results are found in Tables 4 & 5.

DocuSign Envelope ID: 38D0E95E-DD99-44C8-8D42-44CE83DC948B

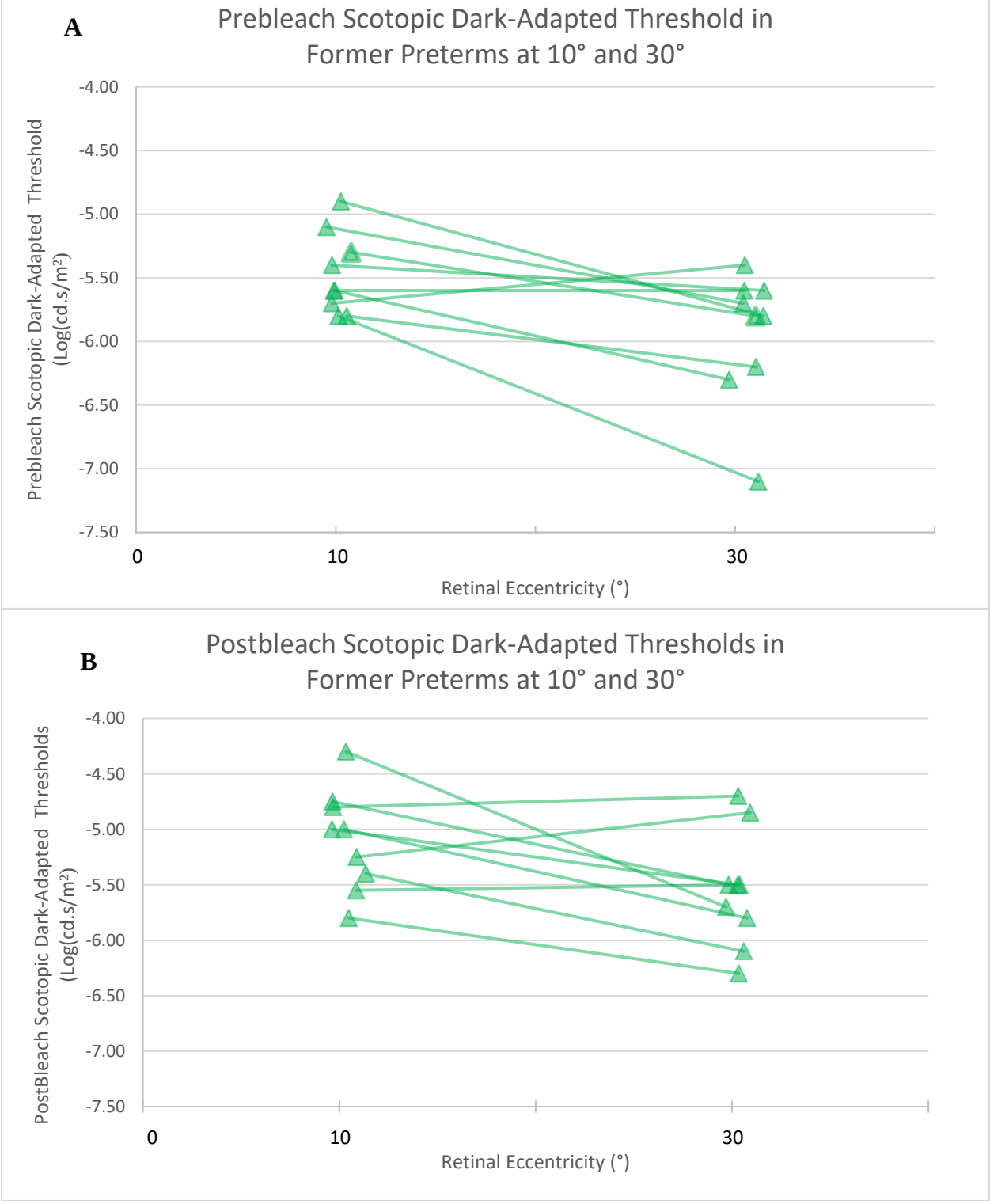

Figure 9: Prebleach and postbleach rod mediated dark-adapted thresholds in former preterms at 10° and 30°

(A) Prebleach and **(B)** postbleach rod mediated dark-adapted thresholds in former preterms at 10° and 30°. Participants who completed both test eccentricities are represented by filled symbols connected by a line.

DocuSign Envelope ID: 38D0E95E-DD99-44C8-8D42-44CE83DC948B

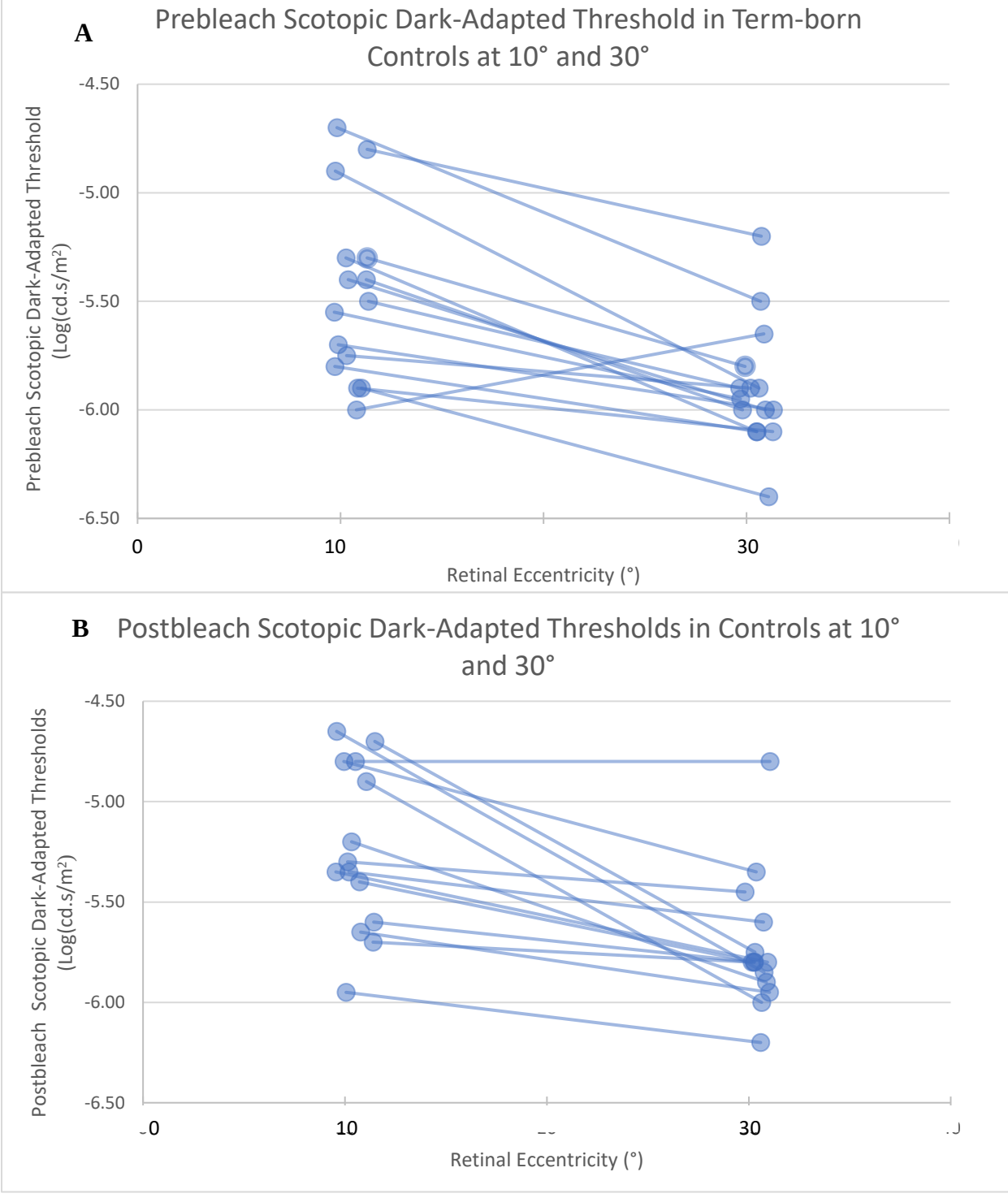

Figure 10: Prebleach and postbleach rod mediated dark-adapted thresholds in term-born controls at 10° and 30°

(A) Prebleach and **(B)** postbleach rod mediated dark-adapted thresholds in term-born controls at 10° and 30°. Participants who completed both test eccentricities are represented by filled symbols connected by a line.

DocuSign Envelope ID: 38D0E95E-DD99-44C8-8D42-44CE83DC948B

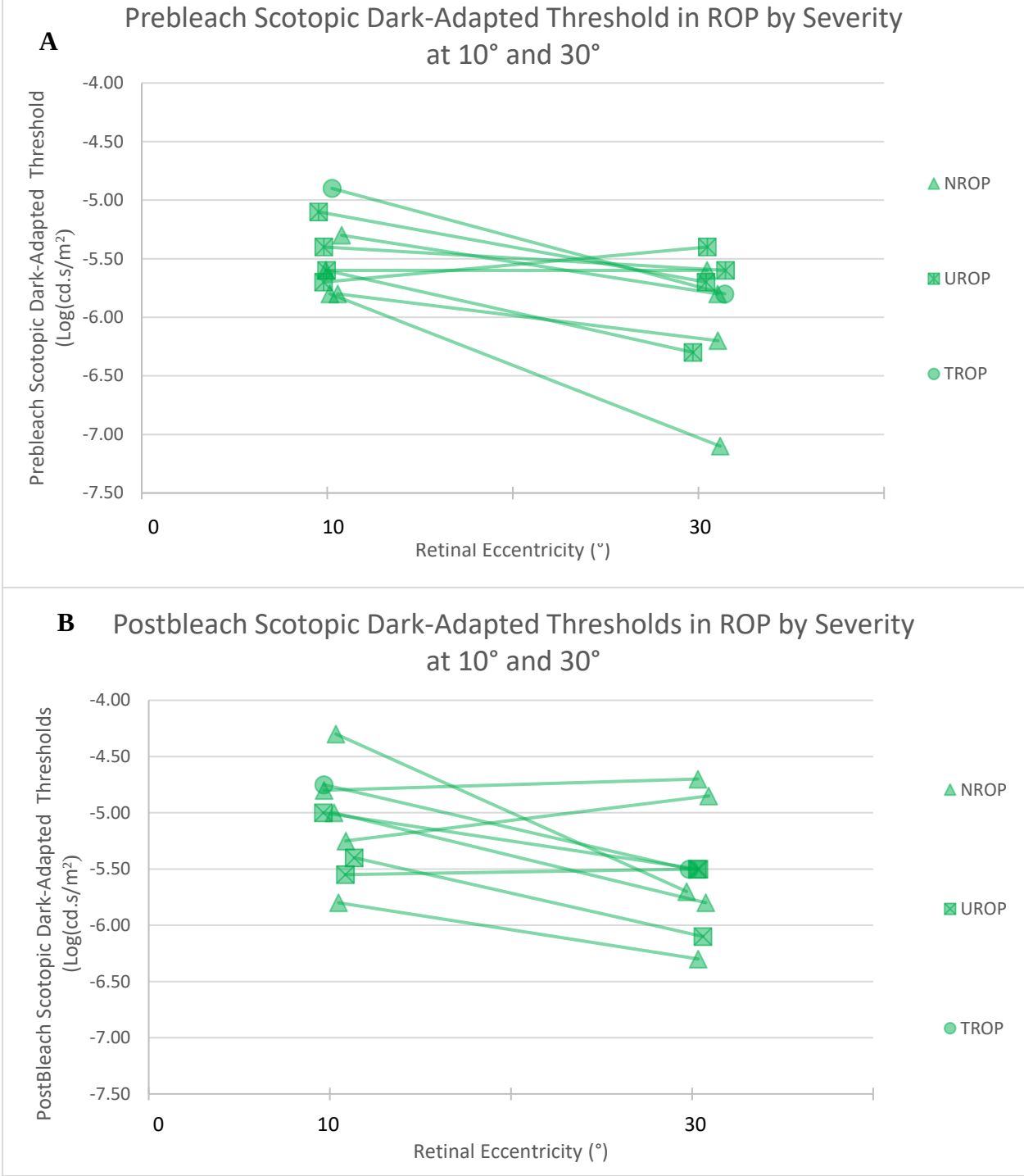

Figure 11: Prebleach and postbleach rod mediated dark-adapted thresholds in former preterms by ROP severity at 10° and 30°

(A) Prebleach and **(B)** postbleach rod mediated dark-adapted thresholds in former preterms by ROP severity at 10° and 30° retinal eccentricities Participants who completed both test eccentricities are represented by filled symbols connected by a line. Different symbols indicate the severity of ROP in the former preterms.

DocuSign Envelope ID: 38D0E95E-DD99-44C8-8D42-44CE83DC948B

Table 4: ANOVA of prebleach rod mediated dark-adapted thresholds

Source	Sum of Squares	df	Mean Square	F	Sig.
Group (Former preterms, Term-born controls)	0.006	1	0.006	0.028	0.868
Eccentricity (10°, 30°)	2.294	1	2.294	28.715	<0.001*
Group x **Eccentricity**	0.002	1	0.002	0.030	0.865

Statistical significant is denoted by * ($\alpha = 0.05$).

Table 5: ANOVA of postbleach rod mediated dark-adapted thresholds

Source	Sum of Squares	df	Mean Square	F	Sig.
Group (Former preterms, Term-born controls)	0.268	1	0.268	1.053	0.317
Eccentricity (10°, 30°)	2.390	1	2.390	22.580	<0.001*
Group x **Eccentricity**	0.001	1	0.001	0.014	0.908

Statistical significant is denoted by * ($\alpha = 0.05$).

3.3 Cone Mediated Dark-Adapted Thresholds

Although the focus of our research is on rod function, the ColorDome also collects data on cone mediated function. There was no significant difference between former preterms and term born controls for prebleach and postbleach cone mediated dark-adapted thresholds. Similar to rod mediated findings, there was a significantly lower threshold response at 30°, in both prebleach (p=0.00034) and postbleach (p=0.00011) cone mediated dark-adapted thresholds in all participants.

4. General Discussion and Conclusions

4.1 Summary of Key Findings

To our knowledge, our project is the first to study S2 rod mediated function at two different retinal eccentricities in the same former preterm participant. Our results show that S2 values, indicating the rate of rod mediated recovery of visual sensitivity, did not differ between former preterms and term-born controls. The retinal eccentricity 10° and 30°, had no significant

DocuSign Envelope ID: 38D0E95E-DD99-44C8-8D42-44CE83DC948B

effect on S2 values. The severity of antecedent ROP did not have a significant effect on S2 values. We had hypothesized that in former preterms with a history of early high myopia would be associated with slow kinetics of rod mediated recovery of sensitivity. Unfortunately, we did not have participants with these characteristics and thus could not test this hypothesis. COVID restrictions affected recruitment, and this impacted many aspects of our study, particularly the recruitment and scheduling of former preterms with early high myopia. These are the most frafile and least numerous of our cohort of former preterms.

4.2 S2 rod mediated recovery

We found S2, rod mediated recovery of sensitivity in former preterms was the same compared to term-born controls at 10° and 30°. This S2 result is evidence that 11- cis retinal (chromophore) in the retinal pigment epithelium is delivered to rhodopsin (opsin) in the disc of the rod outer segment (Lamb, 1981; Lamb and Pugh, 2004; Palczewski, 2006). S2 has three distinct components. First, the recovery of threshold against time has a constant slope for bleach ranging from 1-100% bleach (Lamb and Pugh, 2004). Second, in small bleaches (<20% bleach) the recovery shifted right in logarithmic increments per unit bleach (Lamb and Pugh, 2004). Lastly, for larger bleaches (>10-20%), the curve also shifted right by proportional to the initial bleach strength (Lamb and Pugh, 2004).

The composition of our former preterms included eight NROP, seven UROP, and one TROP, but none had early high myopia. Early high myopia is found among TROP and occasionally UROP. We look forward to adding former preterms with a history of early high myopia to the sample. We predict those with early high myopia will have slower S2 function as has been found in some retinal diseases. Significantly slower S2 function has been documented in rod affected retinal diseases such as Stargardt's, age related macular degeneration, vitamin A

DocuSign Envelope ID: 38D0E95E-DD99-44C8-8D42-44CE83DC948B

deficiency, and Fundus Albipuncta (Blakemore and Rushton, 1965; Glenn et al., 1994, Cideciyan *et al.*, 2004). Each of these disorders have abnormal retinal pigment epithelium and rod outer segment interactions.

Bowl et al., (2019) found slower S2 in former preterms ages 6 to 13 years old with and without a history of ROP. They compared macular OCT findings with S2 function. They suggested former preterms with an abnormal ratio of the outer nuclear layer to inner retinal layers at the fovea; termed macular development arrest, had slower S2 rod mediated recovery (Bowl et al., 2019). Unfortunately, OCTs were not explored in our study so we cannot directly compare results.

4.3 S2 Rod Mediated Recovery Literature Comparison

We compared our experimental control S2 data to the literature to see if our data was consistent with the literature. We compared our experimental control S2 data to the literature by stimulus size and retinal eccentricity. There was a significant range of literature S2 spanning from 0.43 to 5º test stimulus diameter (Figure 12). The range of the reported S2 by Owsley et al., (2001), and Tahir et al., (2017) at 2º diameter size overlaps with most of our experimental controls. Based on stimulus size, our S2 stimulus size parameter was within reasonable agreement with the literature.

We tested the same participants at 10º and 30º. Literature S2 has been reported at a single retinal eccentricity shown in Figure 13. There was a range of tested retinal eccentricity spanning from 3° to 30°. Compared to the literature values, our term-born S2 at 10º is within the range of reported S2 from 3 to 13.4º. There was only one literature S2 value at the time of this study that can be compared to our term-born S2 at 30º. This S2 value reported by Cideciyan et al., (1997)

DocuSign Envelope ID: 38D0E95E-DD99-44C8-8D42-44CE83DC948B

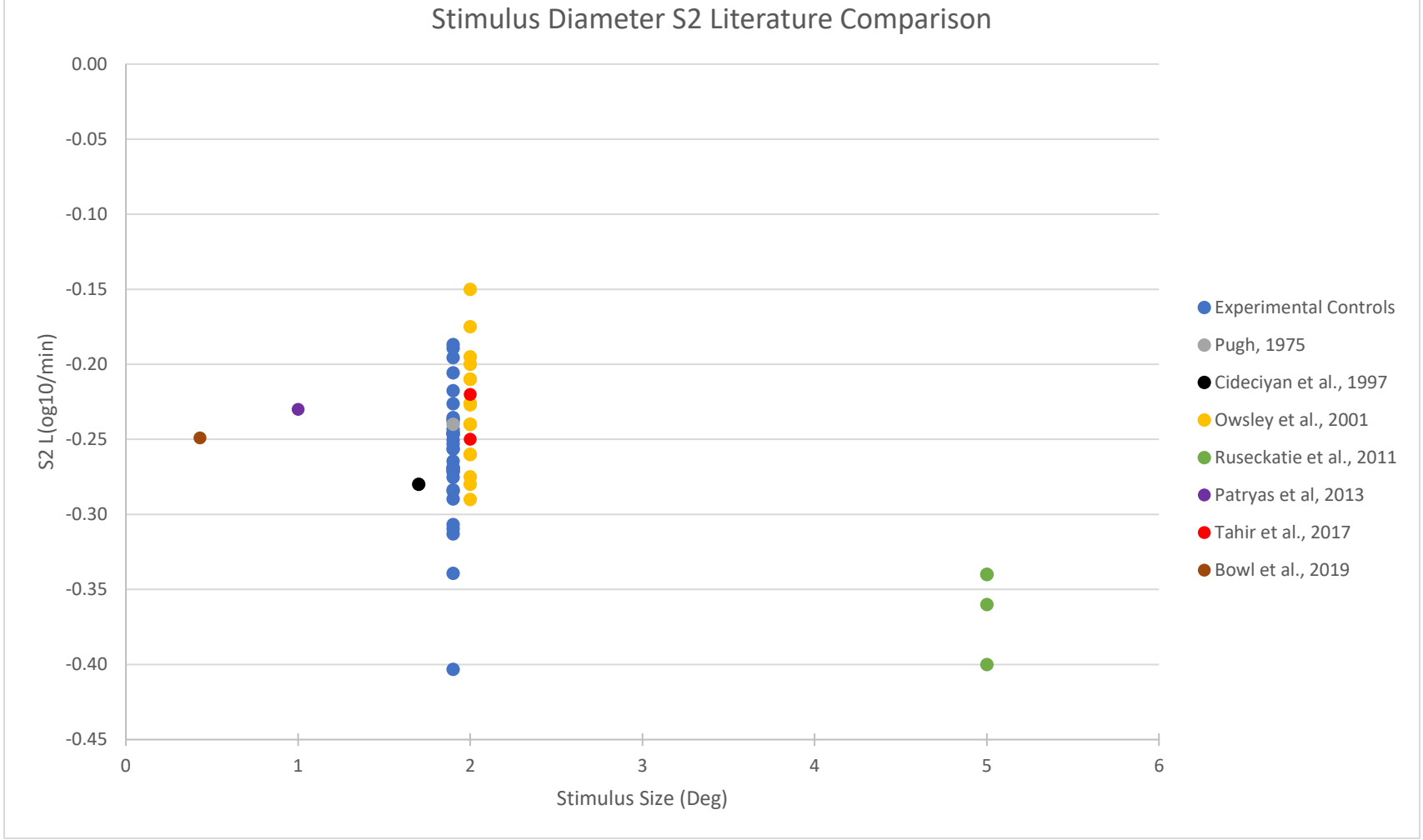

Figure 12: Stimulus Diameter S2 Literature Comparison

Comparison of experimental S2 stimulus size parameter to other literature normal controls. There was significant overlap at the 2 deg stimulus size by experimental controls, Owsley et al., 2001, and Tahir et al., 2017. Experimental controls were presented stimulus size of 2 deg, but for viewing purposes have been shifted left by 0.1 deg.

DocuSign Envelope ID: 38D0E95E-DD99-44C8-8D42-44CE83DC948B

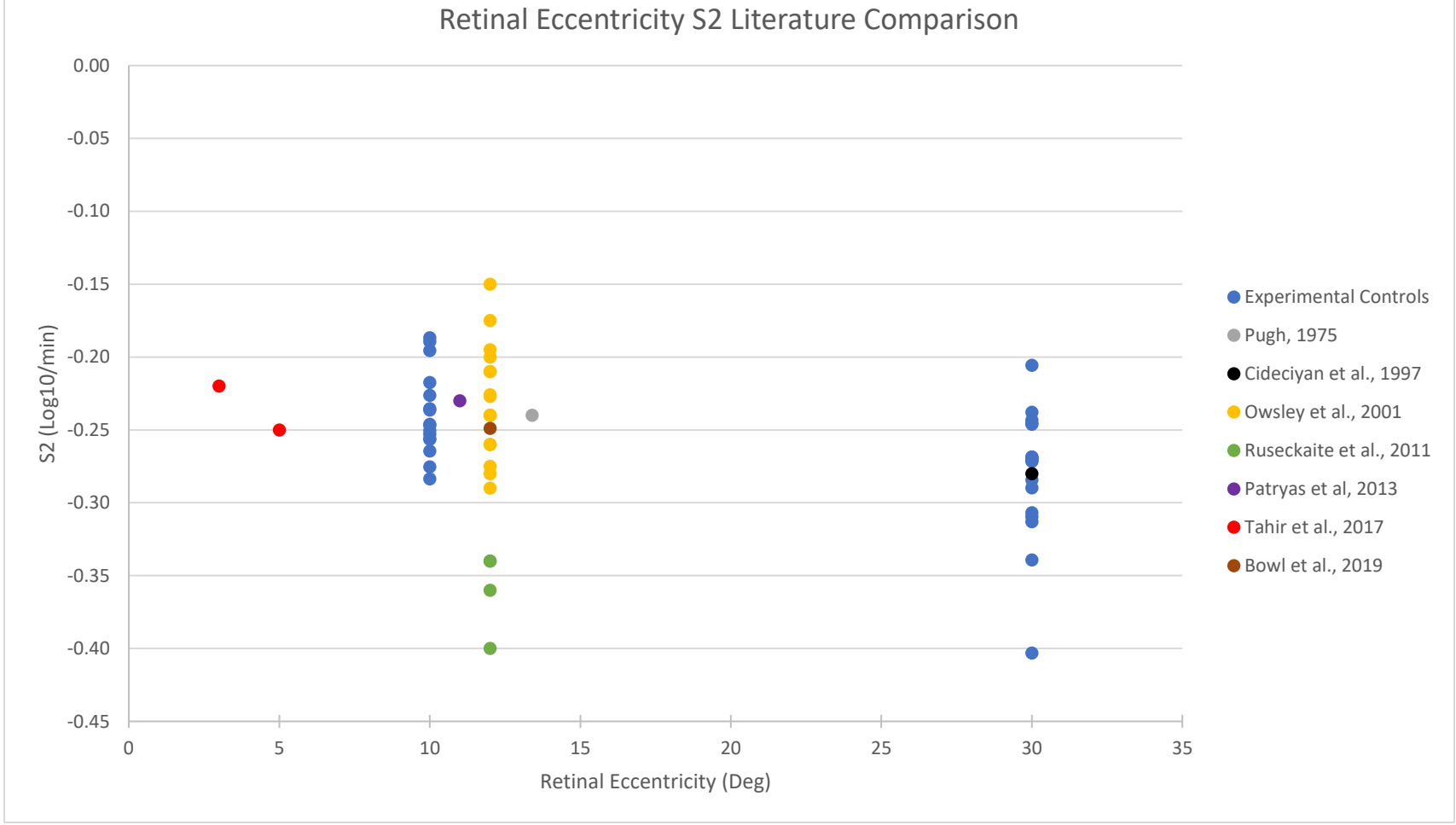

Figure 13: Retinal Eccentricity S2 Literature Comparison

Comparison of experimental S2 tested retinal eccentricity with literature normal controls.

DocuSign Envelope ID: 38D0E95E-DD99-44C8-8D42-44CE83DC948B

was within our range of S2. Overall, our experimental protocol parameters are consistent with literature S2 values based on stimulus diameter and retinal eccentricity (Pugh, 1975; Cideciyan *et al.,* 1997; Owsley *et al.,* 2001; Ruseckatie *et al.,* 2011; Patryas *et al.,* 2013; Tahir *et al.,* 2017; Bowl *et al*., 2019).

4.4 Rod Mediated Thresholds Between Preterms and Term-born Controls

There was no difference between rod mediated dark-adapted thresholds between former preterms and term-born controls. This finding was consistent given the composition of our former preterms being majority NROP. Previous ERG studies have shown reduced rod photoreceptor sensitivity in UROP and TROP in infancy compared to term-born subjects (Fulton et al., 2009 a). When participants were tested again in childhood after active ROP has resolved, the post-receptor function was normal in UROP but not TROP (Fulton *et al.,* 2009 a).

Another ERG study demonstrated that UROP had affected photoreceptor function as infants but near normal post-receptor function, b-wave sensitivity and visual threshold as children (Harris *et al.,* 2011). TROP demonstrated both abnormal photoreceptor and post-receptor abnormalities both as infants and children (Harris *et al.,* 2011). Although UROP and TROP have demonstrated affected rod photoreceptor function in infancy, abnormal rod function only persists in TROP.

Affected rod photoreceptor functions seen in individuals with a history of ROP, this led us to suspect there may be higher rod mediated thresholds in UROP and or TROP (Fulton *et al.,* 2009 a). NROP, were expected to act like term-born controls (Barnaby *et al.,* 2007; Hansen *et al.,* 2017). As the majority of our former preterms were composed of NROP, it makes sense that there was little to no difference seen between groups. If more TROP were included in our sample, there may or may not be a difference between groups.

DocuSign Envelope ID: 38D0E95E-DD99-44C8-8D42-44CE83DC948B

4.5 Rod Mediated Thresholds Between 10° and 30°

Dark-adapted rod mediated thresholds were significantly higher at 10° compared to 30° in all participants. We expected term-born controls to have no difference between 10° and 30° (Massof *et al.,* 1981; Hansen and Fulton, 1999; Fulton *et al.*, 2009 b). In former preterms, Reisner et al. found higher dark-adapted thresholds at 10° in resolved ROP children who were highly myopic (≥ -5.00 diopters) by eighteen months of age but thresholds at 30° where within norms (1997). Previous dark-adapted studies using preferential looking in infants have shown higher threshold maturation at 10° compared to 30° but resolved by two years of age if they did not develop early myopia (Barnaby et al., 2007). These persistent higher thresholds in ROP are commonly seen in highly myopic ROP individual, which none of our former preterms are. A combination of factors can contribute to higher thresholds including pupil diameter, light adaptation of receptors, post-receptor light adaptation, and presentation of rod favored, and cone favored stimuli (Reeves and Grayhem, 2016).

The study protocol was designed to alternate rod and cone favored stimulus presentations. There was a possibility of a spillover effect from the cone favored stimulus affecting the final rod mediated dark-adapted thresholds and vice versa. To study the individual rod mediated and cone mediated effects, only one stimulus color should be presented to avoid potential spillover effects.

4.6 Cone Mediated Thresholds

Cone mediated dark-adapted thresholds findings were similar to rod mediated threshold findings. There was no statistical difference between groups. This finding was expected as ROP primarily affected rod function and not cone. (Fulton *et al.,* 2009 a). Photoptic dark-adapted thresholds at 10° was higher compared to 30° in all participants. There was little literature at the

DocuSign Envelope ID: 38D0E95E-DD99-44C8-8D42-44CE83DC948B

time of this study, looking at the effects of cone dark-adapted thresholds and retinal eccentricity. Historical experiment has suggested an increased parafoveal cone sensitivity compared to the peripheral retina (Drum, 1980). However, there could also be one log unit range of thresholds collected at one retinal eccentricity (Massof *et al.*, 1981). In this study, we primarily focused on rod function. Studies have suggested to use different bleaching methods to study the individual effects of rod and cone function (Dimitrov *et al.*, 2012, and Dimitrov *et al.*, 2011). More refined testing parameters would be needed to future explore specific cone mediated function.

4.7 Limitations of the study

One limitation of this study was the small sample size of former preterms; especially, recruitment of TROP individuals. Several factors contributed to this, including the difficultly of recruiting medically stable former preterms and the COVID-19 pandemic. TROPs may have other lifelong complications that excluded them from the study including, neurological impairment, cognitive delay, and brain injury (Cavallaro *et al.*, 2014). The COVID-19 pandemic has also significantly affected recruitment of all participants. We had subjects scheduled to participate in our study, but due to the nature of the pandemic, many sessions had to be cancelled or rescheduled.

Another limitation of this study was the two-test session of the study to test 10° and 30°. One test session could last up to two hours. As a result, testing at both 10° and 30° on the same day was not feasible. Some participants were lost to follow up, no longer interested, had scheduling conflicts, moved, and/or logistic difficulties due to the COVID-19 pandemic.

4.8 Strengths

In this project, we were able to successfully test former preterms and term born controls at two retinal eccentricities. This would be the first to our knowledge that dark adaptation has

DocuSign Envelope ID: 38D0E95E-DD99-44C8-8D42-44CE83DC948B

been tested at different retinal eccentricities in the same participant. Another strength is that we were able to study dark adaptation in a substantial number of former preterms and term born controls during a pandemic.

Through this project we demonstrated the feasibility of studying dark adaptation and vast information that can be studied including recovery of rod mediated sensitivity, rod mediated thresholds, and cone mediated thresholds. Dark adaptation testing parameters can be adjusted to study rod or cone specific function.

4.9 General Conclusion

In this study, we did not find a significant difference between former preterms and term-born controls for S2 rod mediated recovery. The composition of our former preterms was mainly NROPs whom we expected to act like term-born controls, and we did not have any former preterms with a history of early high myopia. The rejection of our hypothesis is consistent with the finding.

Future branches on this project would focus on former preterms with a history of early high myopia. This particular group of former preterms had demonstrated persistent rod photoreceptor dysfunction in previous psychophysical and ERG experiments. Comparison to neurosensory retina, retinal pigment epithelium, or choroidal thickness using wide-field OCT would also be of consideration.

There is a clinical application in studying dark adaptation and the interaction between the retinal pigment epithelium and rod photoreceptor outer segment in a ROP eye. Studying dark adaptation contributes to the current understanding of how rod photoreceptor functions are affected in ROP. Dark adaptation and recovery of rod mediated sensitivity could be used as a

DocuSign Envelope ID: 38D0E95E-DD99-44C8-8D42-44CE83DC948B

non-invasive test to monitor potential therapeutic interventions. A large-scale investigation into the kinetics would further characterize the persistent effect of ROP on S2, rod mediated retinal function.

DocuSign Envelope ID: 38D0E95E-DD99-44C8-8D42-44CE83DC948B

5. Bibliography

Akula JD, Hansen RM, Martinez-Perez M, Fulton AB. Rod photoreceptor function predicts blood vessel abnormality in retinopathy of prematurity. *Invest Ophthalmol Vis Sci*. 2007;48(9):4351-4359.

Anderson MF, Ramasamy B, Lythgoe DT, Clark D. Choroidal thickness in regressed retinopathy of prematurity. *Eye*. 2014;28(12):1461-1468.

Barnaby AM, Hansen RM, Moskowitz A, Fulton AB. Development of scotopic visual thresholds in retinopathy of prematurity. *Invest Ophthalmol Vis Sci*. 2007;48(10):4854-4860.

Blakemore CB, Rushton WA. The rod increment threshold during dark adaptation in normal and rod monochromat. *J Physiol*. 1965;181(3):629-640.

Bowl W, Lorenz B, Stieger K, Schweinfurth S, Holve K, Andrassi-Darida M. Fundus-controlled dark adaptometry in young children without and with spontaneously regressed retinopathy of prematurity. *Trans Vis Sci Tech*. 2019;8(3):62-62.

Cavallaro G, Filippi L, Bagnoli P, et al. The pathophysiology of retinopathy of prematurity: An update of previous and recent knowledge. *Acta Ophthalmol*. 2014;92(1):2-20.

Cideciyan AV, Pugh EN, J., Lamb TD, Huang Y, Jacobson SG. Rod plateaux during dark adaptation in sorsby's fundus dystrophy and vitamin A deficiency. *Invest Ophthalmol Vis Sci*. 1997;38(9):1786-1794.

Cideciyan AV, Aleman TS, Swider M, et al. Mutations in ABCA4 result in accumulation of lipofuscin before slowing of the retinoid cycle: A reappraisal of the human disease sequence. *Hum Mol Genet*. 2004;13(5):525-534.

Chan-Ling T, Gole GA, Quinn GE, Adamson SJ, Darlow BA. Pathophysiology, screening and treatment of ROP: A multi-disciplinary perspective. *Prog Retin Eye Res*. 2018;62:77-119.

Chiang MF, Quinn GE, Fielder AR, et al. International classification of retinopathy of prematurity, third edition. *Ophthalmology*. 2021;128(10):e51-e68.

Darwish D, Chee R, Patel SN, et al. Anti-vascular endothelial growth factor and the evolving management paradigm for retinopathy of prematurity. *The Asia-Pacific Journal of Ophthalmology*. 2018;7(3).

Diagnosys [Package insert]. Lowell; Diagnosys LLC: 2021

Dimitrov PN, Robman LD, Varsamidis M, et al. Visual function tests as potential biomarkers in age-related macular degeneration. *Invest Ophthalmol Vis Sci*. 2011;52(13):9457-9469.

Dimitrov PN, Robman LD, Varsamidis M, et al. Relationship between clinical macular changes and retinal function in age-related macular degeneration. *Invest Ophthalmol Vis Sci*. 2012;53(9):5213-5220.

Drum B. Cone threshold vs. retinal eccentricity: Changes with dark adaptation. *Invest Ophthalmol Vis Sci*. 1980;19(4):432-435.

Enríquez AB, Avery RL, Baumal CR. Update on anti-vascular endothelial growth factor safety for retinopathy of prematurity. *The Asia-Pacific Journal of Ophthalmology*. 2020;9(4).

Fierson WM, AMERICAN ACADEMY OF PEDIATRICS Section,on Ophthalmology, AMERICAN ACADEMY OO, et al. Screening examination of premature infants for retinopathy of prematurity. *Pediatrics*. 2018;142(6).

DocuSign Envelope ID: 38D0E95E-DD99-44C8-8D42-44CE83DC948B

Fulton AB, Hansen RM, Dorn E, Henderickson AE. Development of primate rod structure and function. In: Vital-Durand F, Atkinson J, Braddick OJ, eds. *Infant vision*. Oxford: Oxford University press; 1996:33-49

Fulton AB, Hansen RM. Photoreceptor function in infants and children with a history of mild retinopathy of prematurity. *J Opt Soc Am A*. 1996; 13:566-571.

Fulton AB, Dodge J, Hansen RM, Williams TP. The rhodopsin content of human eyes. *Invest Ophthalmol Vis Sci*. 1999;40(8):1878-1883.

Fulton AB, Hansen RM, Moskowitz A, Akula JD. The neurovascular retina in retinopathy of prematurity. *Prog Retin Eye Res*. 2009 a;28(6):452-482.

Fulton, Anne, Hansen, Ronald, Moskowitz, Anne. Development of Rod Function in Term Born and Former Preterm Subjects. *Optom Vis Sci*. 2009 b;86(6):E653-E658.

Gantz MG, Carlo WA, Finer NN, et al. Achieved oxygen saturations and retinopathy of prematurity in extreme preterms. *Archives of disease in childhood.Fetal and neonatal edition*. 2020;105(2):138-144.

Glass HC, Costarino AT, Stayer SA, Brett CM, Cladis F, Davis PJ. Outcomes for extremely premature infants. *Anesth Analg*. 2015;120(6):1337-1351.

Glenn AM, Fishman GA, Gilbert LD, Derlacki DJ. Effect of vitamin A treatment on the prolongation of dark adaptation in stargardt's dystrophy. *Retina*. 1994;14(1):27-30.

Hansen RM, Fulton AB. The course of maturation of rod-mediated visual thresholds in infants. *IOVS*. 1999;40(8):1883-1886.

Hansen RM, Fulton AB. Dark-adapted thresholds at 10 and 30 deg eccentricities in 10 week-old infants. *Vis Neurosci*. 1995;12(3):509-512.

Hansen RM, Moskowitz A, Akula JD, Fulton AB. The neural retina in retinopathy of prematurity. *Progress in Retinal and Eye Research*. 2017;56:32-57.

Hardy RJ, Good WV, Dobson V, et al. The early treatment for retinopathy of prematurity clinical trial: Presentation by subgroups versus analysis within subgroups. *Br J Ophthalmol*. 2006;90(11):1341.

Harris ME, Moskowitz A, Fulton AB, Hansen RM. Long-term effects of retinopathy of prematurity (ROP) on rod and rod-driven function. *Documenta Ophthalmologica*. 2011;122(1):19-27.

Hecht S, Haig C, Chase AM. The influence of light adaptation on subsequent dark adaptation of the eye. *J Gen Physiol*. 1937;20(6):831-850.

Hendrickson A., Drucker D. The development of parafoveal and mid-peripheral human retina. *Behavioural Brain Research*. 1992; 49(1)21-31.

Jackson GR, Owsley C, McGwin G. Aging and dark adaptation. *Vision Research*. 1999;39(23):3975-3982.

Jacobson L, Vollmer, B., Böhm, B., Kistner, A.. Severity of retinopathy of prematurity was associated with a higher risk of cerebral dysfunction in young adults born extremely preterm; severity of retinopathy of prematurity was associated with a higher risk of cerebral dysfunction in young adults born extremely preterm. *Acta Paediatrica, International Journal of Paediatrics*. 2021;110(2):528-536.

Jang JH, Kim YC. Retinal vascular development in an immature retina at 33-34 weeks postmenstrual age predicts retinopathy of prematurity. *Sci Rep*. 2020;10(1):18111-020-75151-0.

DocuSign Envelope ID: 38D0E95E-DD99-44C8-8D42-44CE83DC948B

Kawamura S, Tachibanaki S. Rod and cone photoreceptors: Molecular basis of the difference in their physiology. *Comparative Biochemistry and Physiology Part A: Molecular & Integrative Physiology*. 2008;150(4):369-377.

Khosnoud Shariati M, Fallahi M, Taslimi Taleghani N, Zonubi M, Dastijani Farahani A. Evaluation of risk factors for retinopathy of prematurity in preterm neonates. *IJN*. 2019;10(1):23-30.

Kong L, Fry M, Al-Samarraie M, Gilbert C, Steinkuller PG. An update on progress and the changing epidemiology of causes of childhood blindness worldwide. *Journal of American Association for Pediatric Ophthalmology and Strabismus*. 2012;16(6):501-507.

Lamb TD. The involvement of rod photoreceptors in dark adaptation. *Vision Res*. 1981;21(12):1773-1782.

Lamb TD, Pugh EN. Dark adaptation and the retinoid cycle of vision. *Prog Retin Eye Res*. 2004;23(3):307-380.

Lee H, Purohit R, Patel A, et al. In vivo foveal development using optical coherence tomography. *Invest Ophthalmol Vis Sci*. 2015;56:4537-4545

Leibrock CS, Reuter T, Lamb TD. Molecular basis of dark adaptation in rod photoreceptors. *Eye*. 1998;12(3):511-520.

Mahroo OAR, Lamb TD. Recovery of the human photopic electroretinogram after bleaching exposures: Estimation of pigment regeneration kinetics. *J Physiol (Lond)*. 2004;554(2):417-437.

Massof RW, Johnson MA, Finkelstein D. Peripheral absolute threshold spectral sensitivity in retinitis pigmentosa. *Br J Ophthalmol*. 1981;65(2):112.

Owsley C, McGwin G, Clark ME, et al. Delayed rod-mediated dark adaptation is a functional biomarker for incident early age-related macular degeneration. *Ophthalmology*. 2016;123(2):344-351.

Palczewski K. G protein-coupled receptor rhodopsin. *Annu Rev Biochem*. 2006;75:743-767

Patryas L, Parry NRA, Carden D, et al. Assessment of age changes and repeatability for computer-based rod dark adaptation. *Graefe's Archive for Clinical and Experimental Ophthalmology*. 2013;251(7):1821-1827.

Provis JM, Hendrickson AE. The foveal avascular region of developing human retina. *Arch Ophthalmol*. 2008;126(4):507-511.

Pugh EN. Rushton's paradox: Rod dark adaptation after flash photolysis. *J Physiol (Lond)*. 1975;248(2):413-431.

Reeves A, Grayhem R. Role of extrinsic noise in the sensitivity of the rod pathway: Rapid dark adaptation of nocturnal vision in humans. *J Opt Soc Am A*. 2016;33(3):351-360.

Reisner DS, Hansen RM, Findl O, Petersen RA, Fulton AB. Dark-adapted thresholds in children with histories of mild retinopathy of prematurity. *IOVS*. 1997;38(6):1175-1183.

Repka MX, Palmer EA, Tung B, for the Cryotherapy for Retinopathy of Prematurity,Cooperative Group. Involution of retinopathy of prematurity. *Arch Ophthalmol*. 2000;118(5):645-649.

Reuter T. Fifty years of dark adaptation 1961–2011. *Vision Res*. 2011;51(21):2243-2262

Ruseckaite R, Lamb TD, Pianta MJ, Cameron AM. Human scotopic dark adaptation: Comparison of recoveries of psychophysical threshold and ERG b-wave sensitivity. *J Vis*. 2011;11(8):1-16.

DocuSign Envelope ID: 38D0E95E-DD99-44C8-8D42-44CE83DC948B

691 Sayman Muslubas I, Karacorlu M, Hocaoglu M, Arf S, Ozdemir H. Retinal and choroidal
692 thickness in children with a history of retinopathy of prematurity and transscleral diode
693 laser treatment. *Eur J Ophthalmol*. 2017;27(2):190-195.
694 Stahl A, Krohne TU, Eter N, et al. Comparing alternative ranibizumab dosages for safety and
695 efficacy in retinopathy of prematurity: A randomized clinical trial. *JAMA Pediatr*.
696 2018;172(3):278-286.
697 Tahir HJ, Rodrigo-Diaz E, Parry NRA, Kelly JMF, Carden D, Murray IJ. Slowed dark
698 adaptation in older eyes; effect of location. *Exp Eye Res*. 2017;155:47-53.